ChemComm

COMMUNICATION

View Article Online
View Journal | View Issue

Cite this: *Chem. Commun.*, 2025, **61**, 18629

Received 2nd September 2025,
Accepted 20th October 2025

DOI: 10.1039/d5cc04931h

rsc.li/chemcomm

A series of three liquid crystalline cubic phases with an alternating sequence of single- and double-network structures

Silvio Poppe,[a] Changlong Chen,[b] Matthias Wagner,[a] Yu Cao, *[bc] Feng Liu [bc] and Carsten Tschierske *[a]

Bolapolyphiles, built of a π-conjugated bistolane core with polar glycerol groups at each end and two linear alkyl side-chains in lateral positions form a series of three different cubic network phases upon side-chain elongation, the single network "Plumber's nightmare" (*Pm*$\bar{3}$*m*, SP), the double gyroid (*Ia*$\bar{3}$*d*, DG) and the single diamond network phase (*Fd*$\bar{3}$*m*, SD) with the DG as an intermediate phase at the SP to SD transition.

Networks describe patterns of connection in many natural and artificial systems and are of significant interest as the basis of communication and data processing systems.[1] Self-assembled supramolecular networks can transmit matter or information through space, as for example, charge carriers[2,3] or chirality information.[4] If the nodes and edges of such networks are arranged in periodic structures they can be applied as photonic crystals[5,6] and the resulting spaces in the network meshes can find use for catalysis, storage and separation purposes.[7] Liquid crystalline (LC) networks, commonly known as bicontinuous cubic phases, are structures occurring in small ranges at the transition between lamellar and columnar self-assembly of amphiphiles, as found in lyotropic (mostly aqueous) surfactant and lipid systems,[8,9] in block-copolymer morphologies[10] and in some LC phases of polyaromatic compounds with long or multiple flexible chains.[11] Most often the double gyroid network (DG) with space group *Ia*$\bar{3}$*d* and trigonal junctions is found in these systems, but also the double diamond (DD, *Pn*$\bar{3}$*m*) with tetrahedral and the double "Plumber's nightmare" (DP, *Im*$\bar{3}$*m*) cubic phase with octahedral six-way junctions are known (Fig. 1a–c).[9,12] Usually they appear in small temperature and composition ranges, which makes their production and investigation challenging. Nevertheless, in some cases DD-DG transitions and in very few rare cases even the complete sequence DP-DD-DG was observed in lyotropic systems[13] and in block copolymers.[14] In contrast to the double networks, the self-assembled single networks are extremely rare[5,6] and only two of them, the SD (*Fd*$\bar{3}$*m*)[15] and the SP (single net "Plumber's nightmare", *Pm*$\bar{3}$*m*),[16] have recently been found (Fig. 1e and f) as thermodynamically driven LC phase structures of precisely designed rod-like bolapolyphiles (BPs) with laterally attached alkyl chains.[17] The SP phase was found for a 4-(phenylethynyl)-tolane ("bistolane" = BT) rod-like compound **1/20** with glycerol end-groups and two linear *n*-eicosanyloxy (*n* = 20) chains fixed at the same side of the middle benzene ring (catechol diether, see formula in Table 1).[16] To understand the effect of side-chain length on SP phase formation, compounds **1/*n*** with shorter and longer chains (*n* = 18, 22 and 30) were synthesized and investigated. Surprisingly, even for this limited series, three LC networks with different cubic space groups were

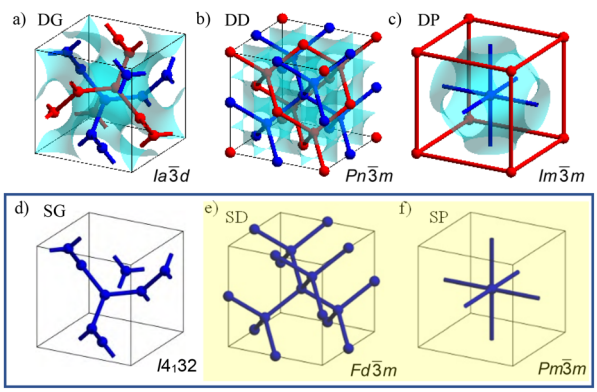

Fig. 1 (a)–(c) Double network cubic phases with corresponding space groups and their infinite minimal surfaces (blue) and (d)–(f) the corresponding single networks. Reproduced from ref. 16.

[a] *Institute of Chemistry, Martin Luther University Halle-Wittenberg, Kurt-Mothes Str. 2, 06120 Halle, Germany. E-mail: Carsten.tschierske@chemie.uni-halle.de*
[b] *Shannxi International Research Center for Soft Matter, State Key Laboratory for Mechanical Behavior of Materials, Xi'an Jiaotong University, Xi'an 710049, P. R. China. E-mail: yu.cao@xjtu.edu.cn*
[c] *Institute of New Concept Sensors and Molecular Materials, Shaanxi Key Laboratory of New Concept Sensors and Molecular Materials, Xi'an Jiaotong University, Xi'an 710049, P. R. China*

Table 1 Data of compounds **1/*n***[a]

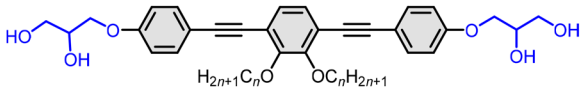

Compd.	Phase transitions (T/°C [ΔH/kJ mol^{-1}])[a]	a/nm (T/°C)	n_{cell}	n_{bundle}	n_{junct}
1/18	H: Cr 93 [48.8] M 97 [5.9] Cub/$Pm\bar{3}m$ 126 [0.8] Iso C: Iso 122 [−0.8] Cub/$Pm\bar{3}m$ 85 [−4.7] M 76 [−63.5] Cr	3.62 (110)	28.2	9.4	56
1/20[16]	H: Cr 98 [74.8] Cub/$Pm\bar{3}m$ 134 [1.0] Iso C: Iso 130 [−1.4] Cub/$Pm\bar{3}m$ 79 [−78.0] Cr	3.61 (100)	26.3	8.7	52
1/22	H: Cr 101 [84.8] Cub/$Ia\bar{3}d$ 148 [1.5] Iso C: Iso 141 [−0.8] Cub/$Ia\bar{3}d$ 78 [−92.5] Cr	9.09 (120)	395.2	16.4	49
1/30	H: Cr 106 [100.6] Cub/$Fd\bar{3}m$ 147 [1.4] Iso C: Iso 139 [−1.2] Cub/$Fd\bar{3}m$ 76 [−116.6] Cr	6.74 (130)	130.6	8.2	33

[a] Determined by DSC (second heating/cooling curves, 10 K min^{-1}, peak temperatures); abbreviations: Cr = crystalline solid, Cub/$Pm\bar{3}m$ = primitive cubic phase (''single Plumber's nightmare'', SP), Cub/$Ia\bar{3}d$ = double gyroid cubic phase (DG), Cub/$Fd\bar{3}m$ = single diamond cubic phase (SD), M = unknown LC phase, see texture in Fig. S2b (SI); Iso = isotropic liquid, H: = data on heating, C: = data on cooling; a = cubic lattice parameter, n_{cell} = molecules per unit cell; n_{bundle} = number of molecules in the cross section of the coaxial rod bundles; n_{junct} = number of glycerols in the polar spheroids; for calculation, see Table S4 and for DSCs see Fig. S1 (SI).

observed, representing the first case of a sequence SP-DG-SD, combining double and single network phases, reported here.

The synthesis (Scheme S1, SI) and analytical data of the new compounds **1/*n*** with n = 18, 22, 30, and the used investigation methods are described in the SI. The observed phase transitions and structural data of the mesophases of all compounds, including **1/20**[16] are collated in Table 1.

Upon cooling from the isotropic liquid state, for all compounds a small exotherm in the DSC traces (ΔH = −0.8 to −1.4 kJ mol^{-1}, see Table 1 and Fig. S1, SI) is an indication of a phase transition within the optically isotropic phase range, which is associated with a significant increase of viscosity after crossing this transition, leading to a viscoelastic isotropic solid (Fig. S2a, SI). Upon heating, this transition is slightly shifted to higher temperature, associated with a transition from the plastic to the fluid isotropic phase with a hysteresis of 4–8 K upon cooling (Fig. S1, SI). In the plastic isotropic mesophase range only one diffuse scattering with a maximum at d = 0.45–0.46 nm is found in the wide-angle X-ray scattering (WAXS) profile for all compounds **1/*n*** (see Fig. S3a, S5a, S7a, SI), indicating a broad distribution of the mean distance between the molecules and molecular segments and the absence of any fixed positions of individual molecules.[11b] In the small-angle (SAXS) range a series of sharp reflections confirm a periodic lattice (Fig. 2a, d, g). Both together support the LC state of this isotropic mesophase, being typical for cubic mesophases.

Three different SAXS patterns were observed for the cubic phases, depending on the chain length (Fig. 2). For compound **1/18** the SAXS patterns can be indexed to a $Pm\bar{3}m$ space group (ratio 1/d-values: $1:\sqrt{3}:\sqrt{4}:\sqrt{5}$, Fig. 2a) with a lattice parameter of a = 3.6 nm, being almost the same as reported for **1/20**.[16] The reconstructed electron density (ED) map of **1/18** (Fig. 2b) shows an electron rich (purple) cubic framework with truncated octahedral (TO) six-way junctions (ν = 6). The framework is formed by the BT units at the edges and the glycerol groups form TO 6-way junctions. The interior of this cubic framework has low ED (not shown for clarity), confirming that this space is completely filled by the low ED alkyl side-chains,

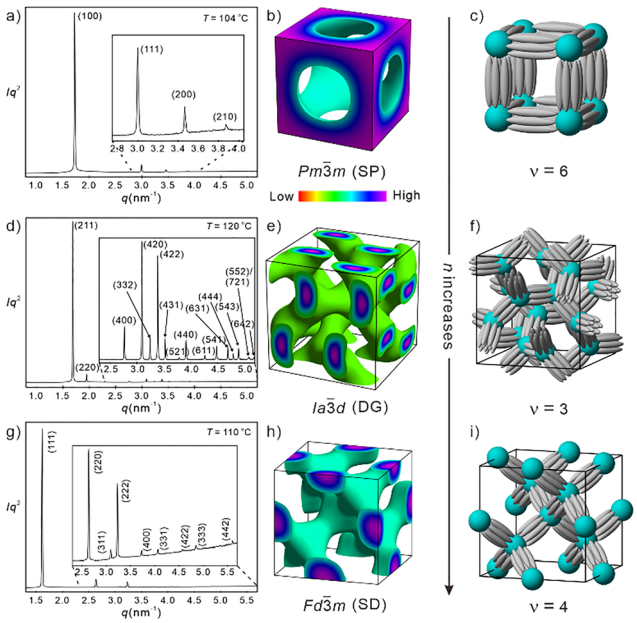

Fig. 2 Cubic phases of **1/*n***, showing a SP-DG-SD transition by side-chain elongation. (a)–(c) SAXS pattern of the SP phase of **1/18** with indexation and the corresponding ED map and model showing the SP network structure, (d)–(f) related data for the DG phase of **1/22**, and (g)–(i) the SD phase of **1/30**; for details and WAXS patterns, see Fig. S3–S8 and Tables S1–S5 (SI).

excluding the possibility of an interpenetration by a second network. This confirms a network formed by fused cube-frames, leading to a simple cubic lattice with octahedral 90° junctions representing a single net of the ''Plumber's nightmare'' (SP, Fig. 2c). Each unit cell is formed by 26.3 molecules, meaning that each edge of the cubic network is formed by coaxial bundles about nine molecules in diameter (n_{bundle} = 9.4). At each junction six edges meet, thus 6 × n_{bundle} = n_{junct} = 56 glycerols form each of the polar polyhedra at the junctions (Table 1), which for simplicity are considered as slightly deformed spheres. This relatively large number of glycerols leads to a significant diameter of these polar

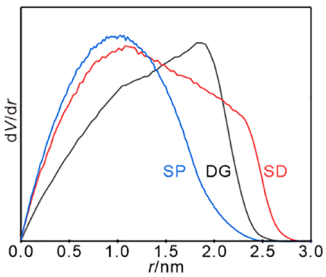

Fig. 3 Radial distribution dV/dr for network phases, where $V(r)$ is the unit cell volume within a distance r from the closest network segment. The intersections of the curves on the x-axis show the furthest distance from the networks in the lattice.

spheres, which contributes to an expansion of the lattice (a_{cub} = d_{nodes} = 3.6 nm), leading to the side length of the cubes being *ca.* 15% longer than the measured molecular length of L_{mol} = 2.8–3.1 nm between the ends of the glycerol groups at the BT rods (Fig. S9, SI). This is in line with the proposed SP structure where only one bundle of coaxial BT-rods lengthwise forms the edges between the glycerol spheres. There is no significant change of the lattice parameter from **1/18** to **1/20**, as it is mainly determined by the molecular (BT-rod) length. Therefore, the slightly smaller number of molecules required to fill the space in the SP lattice of **1/20** leads to a reduction of the number of parallel arranged molecules in the cross-section of the edges from 9.4 for **1/18** to 8.7 for **1/20**.[16]

For the next homologue **1/22** the SAXS pattern changes and another cubic phase, which can be assigned to an $Ia\bar{3}d$ space group (ratio of 1/d-values: $\sqrt{6}{:}\sqrt{8}{:}\sqrt{16}{:}\sqrt{20}{:}\ldots$ *etc.*) with a = 9.1 nm in this case (Fig. 2d). As obvious from the reconstructed ED map (Fig. 2e) two interwoven networks with trigonal three-way junctions have high ED, as typical for double gyroid (DG) cubic network phases. In comparison to the SP structure, the valence of the junctions decreases from ν = 6 to ν = 3 (Fig. 2f). The DG phase is formed by coaxial bundles which in this case consist of n_{bundle} ~16 molecules in the cross section of each network segment, in contrast to only 9 molecules found for SP. Thus, the polar junctions involve 48 glycerols, which is slightly smaller than this number of n_{junct} = 56 (**1/18**) or 52 (**1/20**) of the SP phase (Table 1). The larger number of molecules in the cross section of the edges largely compensates the reduction of the number of attractive hydrogen bonding at the junction by the bisection of the node-valency from 6 to 3. The distance between two adjacent nodes is $d_{nodes} = a_{cub}/(2\sqrt{2})$ = 3.2 nm, which is close to the measured molecular length L_{mol}, meaning that again a single rod-bundle is located lengthwise between the junctions (for exclusion of alternative structures, see Section S2.4, SI). However, the cross section of the bundles formed by 16 molecules must become elliptical in the DG phase (see Fig. 2e) to allow all molecules to submit their chains into the aliphatic continuum. As soon as this deformation crosses a certain limiting value the DG becomes unstable and is replaced by another network type.

Further alkyl chain elongation (compound **1/30**) leads to a $Fd\bar{3}m$ lattice (ratio 1/d-values: $\sqrt{3}:\sqrt{8}:\sqrt{11}:\sqrt{12}:\sqrt{16}{:}\ldots$ *etc.*, see Fig. 2g) with a_{cub} = 6.7 nm. The ED map in Fig. 2h shows a single high ED network with tetrahedral 4-way junctions, as typical for the diamond network (Fig. 2i). The absence of interpenetration leads to the single diamond (SD) structure. Each network segment, which is still formed by only one coaxial molecular bundle in length $(d_{nodes} = \sqrt{3}/4) \cdot a_{cub} = 2.92$ nm[18] is formed by 8 molecules in the cross-section and in this case only about 32 glycerols are organized in the tetrahedral junctions. Thus, the number of glycerols forming the individual nodes decreases from 56–52 in SP *via* 48 in DG to 32 in SD (Table 1).

Overall, the unique phase sequence of three thermotropic cubic network phases Cub/$Pm\bar{3}m$ → Cub/$Ia\bar{3}d$ → Cub/$Fd\bar{3}m$ is found for compounds **1/*n*** with growing chain length from n = 18 to 30. Within the cubic phase sequence, the junction valence is first reduced to one half from 6 to 3 with growing side-chain volume. To allow a sufficient number of hydrogen bondings (glycerols) at the junctions to be stable, they assume an elliptical shape and change the bundle cross-section from circular to elliptical (Fig. 2e). The reduced node valence is also associated with an expansion of the space available between the nets, which leads to a transition from a single to a double network to retain optimized space filling. At the transition of the valence from 3 to 4 with higher network density, the interpenetration is removed again. This experimentally found sequence SP → DG → SD with an alternation of single and double network formation and a local minimum for the junction valence upon side chain expansion coincides with deceasing n_{junct} (Table 1). It is different from the sequence SP → SD → DG predicted by coarse-grain simulation by the position of the DG.[19] This is attributed to the planarity of the trigonal junctions, being the only one allowing elliptical deformation and thus maintaining a larger number of cohesive glycerols at the junctions than SD. Though the phase transition sequence is the same as in Bonnet transformation,[13b] the phase is not controlled by minimal surface transformation. Instead, the phase transition behaves as a result of competition between interfacial tension and space filling.

It is noted that the network phases discussed here are different from the bicontinuous cubic phases formed by molecular and macromolecular amphiphiles, because the networks are not continuous, but segmented into polar (slightly deformed) spheres and rod-bundles with fixed length forming the struts. Two interfaces are generated in these cubic phases; one is between polar glycerols and rigid aromatics and the other is between aromatics and alkyl chains. The interfacial tension is a key factor influencing the cubic network phase behaviour based on SCFT.[20] Minimizing the interfacial tension requires minimization of the interfacial surface area. The aromatic/alkyl interface contributes to the network phase related to the minimal surface. And the glycerol/aromatic interface is defined by network junction shape. Clearly, larger valency induces more spherical junctions, which decreases the interfacial tension and leads to a SP phase as the first network phase and a SD phase upon chain elongation. The DG, usually representing the dominant network phase, is considered as an intermediate structure in this case.

Except for the junction shape, alkyl chain volume also affects the phase behaviour. The experimentally observed sequence SP → DG → SD is in good agreement with predictions based on the development of the radial distribution of the side chain volume dV/dr,[15] where $V(r)$ is the segment of the unit cell volume within a distance r from the closest network segment. Fig. 3 shows the dV/dr curves for the three cubic phases. The SD phase requires longer alkyl chains compared with SP, in line with the molecular design. The intersections between the curves and x-axis give an impression on the furthest distance from the network (Table S5, SI), which reflects the degree of alkyl chain stretching. For SP, the steep increase of the dV/dr curve indicates a rapid volume expansion. Meanwhile, alkyl chains are forced to stretch strongly to fill the free volume. The entropy penalty from alkyl chains stretching competes with the enthalpy gain from the glycerol's size and shape optimization. The entropic penalty lowers the phase stability, generating the lowest Cub-Iso transition point for SP. Upon alkyl chain elongation, DG replaces SP as the alkyl chain entropy penalty can be greatly relieved due to less requirement of chain stretching. Upon further chain elongation, SD becomes a stable phase balancing the junction shape and alkyl chain size.

The fixed length of the relatively long BT rods has an additional effect on network formation. While for compounds with relatively short biphenyl and *p*-terphenyl rods exclusively 3- and 4-way junctions were observed (DG,[21] DD,[22] SD[15]), formation of the SP network with 6-way junctions obviously requires a longer BT core,[16] while the I-WP[23] and A15[24] networks with 8- and 12 + 14-way junctions, respectively, require even longer oligo(phenylene-ethynylene) (OPE) cores involving 5 benzene rings. Similarly, only double networks can be found for biphenyl-based BPs,[21,22] while *p*-terphenyl[15] and BT-based cores[16] allow double as well as single network phases, and for the even longer OPE-based BPs[23,24] only the high valence single networks I-WP and A15 were found so far. For shorter rods, the side chains are closer to the junction points, which limits the possible junction valence due to the arising packing frustration.

In summary, a sequence of three different self-assembled LC network phases was obtained (Fig. 2). Two of them represent the rare single networks (SD, SP), in this case accessible by thermodynamically driven self-assembly in a bottom-up approach. The two single network phases are separated by the double gyroid phase as an intermediate structure at the transition of the junction valence from 6 to 4. Further chain length variations could provide additional new network structures. In particular, elongation beyond n = 30 could possibly lead to the still elusive cubic LC phase with a SG network, which would be of significant interest for energy and environmental science.[25]

This work is supported by the Deutsche Forschungsgemeinschaft (DFG, 346494874-GRK 2670) and the National Natural Science Foundation of China (No. 12204369). We thank the Shanghai Synchrotron Radiation Facility of BL16B1 (https://cstr.cn/31124.02.SSRF.BL16B1) for assistance with SAXS measurements.

Conflicts of interest

There are no conflicts to declare.

Data availability

The data supporting this article have been included as part of the supplementary information (SI). Supplementary information: synthesis, methods, analytical data, additional data and discussions. See DOI: https://doi.org/10.1039/d5cc04931h.

Notes and references

1 M. Newman, *Networks*, Oxford University press, Oxford, 2nd edn, 2018.
2 (*a*) T. Ichikawa, T. Kato and H. Ohno, *Chem. Commun.*, 2019, **55**, 8205; (*b*) T. Kato, J. Uchida, T. Ichikawa and T. Sakamoto, *Angew. Chem., Int. Ed.*, 2018, **57**, 4355.
3 O. Kwon, X. Cai, W. Qu, F. Liu, J. Szydłowska, E. Gorecka, M. J. Han, D. K. Yoon, S. Poppe and C. Tschierske, *Adv. Funct. Mater.*, 2021, 2102271.
4 C. Tschierske and C. Dressel, *Symmetry*, 2020, **12**, 1098.
5 M. Maldovan and E. L. Thomas, *Nat. Mater.*, 2004, **3**, 593.
6 L. Han and S. Che, *Adv. Mater.*, 2018, **30**, 1705708.
7 Y. Ishii, N. Matubayasi, G. Watanabe, T. Kato and H. Washizu, *Sci. Adv.*, 2021, **7**, eabf0669.
8 V. Luzzati, H. Delacroix, A. Gulik, T. Gulik-Krzywicki, P. Mariani and R. Vargas, *Stud. Surf. Sci. Catal.*, 2004, **148**, 17.
9 J. M. Seddon and R. H. Templer, in *Handbook of Biological Physics*, ed. R. Lipowsky and E. Sackmann, Elsevier, 1995, vol. 1, pp. 97–160.
10 (*a*) A. J. Meuler, M. A. Hillmyer and F. S. Bates, *Macromolecules*, 2009, **42**, 7221; (*b*) L. Xiang, Q. Li, C. Li, Q. Yang, F. Xu and Y. Mai, *Adv. Mater.*, 2023, **35**, 2207684; (*c*) H. Lee, J. Kim and M. J. Park, *Phys. Rev. Mat.*, 2024, **8**, 020302.
11 (*a*) S. Kutsumizu, *Isr. J. Chem.*, 2012, **52**, 844; (*b*) G. Ungar, F. Liu and X. B. Zeng, in *Handbook of Liquid Crystals*, ed. J. W. Goodby, P. J. Collings, T. Kato, C. Tschierske, H. F. Gleeson and P. Raynes, Wiley-VCH, Weinheim, 2nd edn, 2014, vol. 5.
12 H. Lee, S. Kwon, J. Min, S.-M. Jin, J. H. Hwang, E. Lee, W. B. Lee and M. J. Park, *Science*, 2024, **383**, 70.
13 (*a*) C. V. Kulkarni, T.-Y. Tang, A. M. Seddon, J. M. Seddon, O. Ces and R. H. Templer, *Soft Matter*, 2010, **6**, 3191; (*b*) C. V. Kulkarni, *Langmuir*, 2011, **27**, 11790.
14 C.-Y. Chang, G.-M. Manesi, C.-Y. Yang, Y. C. Hung, K.-C. Yang, P.-T. Chiu, A. Avgeropoulos and R.-M. Ho, *Proc. Natl. Acad. Sci. U. S. A.*, 2021, **118**, e2022275118.
15 (*a*) X. Zeng, S. Poppe, A. Lehmann, M. Prehm, C. Chen, F. Liu, H. Lu, G. Ungar and C. Tschierske, *Angew. Chem., Int. Ed.*, 2019, **58**, 7375; (*b*) S. Poppe, A. Lehmann, M. Steimecke, M. Prehm, Y. Zhao, C. Chen, F. Liu and C. Tschierske, *Giant*, 2024, **18**, 100254; (*c*) S. Poppe, C. Chen, Y. Cao, F. Liu and C. Tschierske, *Small Sci.*, 2025, **5**, 2500157.
16 S. Poppe, X. Cheng, C. Chen, X. Zeng, R. Zang, F. Liu, G. Ungar and C. Tschierske, *J. Am. Chem. Soc.*, 2020, **142**, 3296.
17 (*a*) C. Tschierske, *Chem. Soc. Rev.*, 2007, **36**, 1930–1970; (*b*) C. Tschierske, C. Nürnberger, H. Ebert, B. Glettner, M. Prehm, F. Liu, X.-B. Zeng and G. Ungar, *Interface Focus*, 2012, **2**, 669.
18 P. M. Duesing, R. H. Templer and J. M. Seddon, *Langmuir*, 1997, **13**, 351.
19 Y. Sun, P. Padmanabhan, M. Misra and F. A. Escobedo, *Soft Matter*, 2017, **13**, 8542.
20 P. Chen, M. K. Mahanthappa and K. D. Dorfman, *J. Polym. Sci.*, 2022, **60**, 2543.
21 (*a*) F. Liu, M. Prehm, X. Zeng, C. Tschierske and G. Ungar, *J. Am. Chem. Soc.*, 2014, **136**, 6846; (*b*) S. Poppe, C. Chen, F. Liu and C. Tschierske, *Chem. Commun.*, 2018, **54**, 11196.
22 X. Zeng, M. Prehm, G. Ungar, C. Tschierske and F. Liu, *Angew. Chem., Int. Ed.*, 2016, **55**, 8324.
23 C. Chen, M. Poppe, S. Poppe, C. Tschierske and F. Liu, *Angew. Chem., Int. Ed.*, 2020, **59**, 20820.
24 (*a*) C. Chen, M. Poppe, S. Poppe, M. Wagner, C. Tschierske and F. Liu, *Angew. Chem., Int. Ed.*, 2022, **61**, e202203447; (*b*) C. Anders, T. Tan, V.-M. Fischer, R. Wang, M. Alaasar, R. Waldecker, Y. Cao, F. Liu and C. Tschierske, *Aggregate*, 2025, **6**, 728.
25 C. Bao, S. Che and L. Han, *J. Hazar. Mater.*, 2021, **402**, 123538.

